AIP | Applied Physics Letters

Diagonal-transition quantum cascade detector

Peter Reininger, Benedikt Schwarz, Hermann Detz, Don MacFarland, Tobias Zederbauer, Aaron Maxwell Andrews, Werner Schrenk, Oskar Baumgartner, Hans Kosina, and Gottfried Strasser

Citation: Applied Physics Letters **105**, 091108 (2014); doi: 10.1063/1.4894767
View online: http://dx.doi.org/10.1063/1.4894767
View Table of Contents: http://scitation.aip.org/content/aip/journal/apl/105/9?ver=pdfcov
Published by the AIP Publishing

Diagonal-transition quantum cascade detector

Peter Reininger,[1,a)] Benedikt Schwarz,[1] Hermann Detz,[1] Don MacFarland,[1] Tobias Zederbauer,[1] Aaron Maxwell Andrews,[1] Werner Schrenk,[1] Oskar Baumgartner,[2] Hans Kosina,[2] and Gottfried Strasser[1]
[1]*Institute for Solid State Electronics and Center for Micro- and Nanostructures, Vienna University of Technology, Vienna, Austria*
[2]*Institute for Microelectronics, Vienna University of Technology, Vienna, Austria*

(Received 29 July 2014; accepted 24 August 2014; published online 4 September 2014)

We demonstrate the concept of diagonal transitions for quantum cascade detectors (QCD). Different to standard, vertical QCDs, here the active transition takes place between two energy levels in adjacent wells. Such a scheme has versatile advantages. Diagonal transitions generally yield a higher extraction efficiency and a higher resistance than vertical transitions. This leads to an improved overall performance, although the absorption strength of the active transition is smaller. Since the extraction is not based on resonant tunneling, the design is more robust, with respect to deviations from the nominal structure. In a first approach, a peak responsivity of 16.9 mA/W could be achieved, which is an improvement to the highest shown responsivity of a QCD for a wavelength of 8 μm at room-temperature by almost an order of magnitude. [http://dx.doi.org/10.1063/1.4894767]

The topic of quantum cascade photodetectors started with the first photovoltaic quantum well infrared photodetector by Schneider *et al.*,[1,2] and the demonstration of a quantum cascade laser as photodetector by Hofstetter *et al.*[3] Graf *et al.*[4,5] and Gendron *et al.*[6,7] established, by specifically designing the quantum cascade structure only for detection, the quantum cascade detector (QCD). QCDs are photodetectors based on intersubband transitions. Two different semiconductor materials form the barriers and the wells, such that, as for all intersubband devices, the transition energy of a QCD can be controlled by designing the thicknesses of the layers. A QCD is a photovoltaic device, i.e., photocurrent is produced without external bias. An asymmetrically designed heterostructure causes a preferential moving direction for excited electron, thereby generating photocurrent. The absorption strength is proportional to the squared dipole matrix element $\langle \chi_i | z | \chi_j \rangle^2$ (DME). Absorption frequencies from the near-infrared to the THz were demonstrated,[8–10] but only in the mid-infrared and near-infrared, room-temperature operation has been reached. Broadband QCDs with response, ranging from about 1100 cm^{-1} to 2000 cm^{-1}, were demonstrated.[11] Photonic crystal cavities have been shown to yield up to four times responsivity enhancement.[12] A quantum cascade device that, under bias voltage, emits and, at zero bias, detects at the same wavelength was reported.[13,14]

In this letter, we present the diagonal transition QCD, a design, where the active transition occurs between two energy levels, each localized in different, but adjacent wells. The same concept has been demonstrated for quantum cascade lasers,[15] by using a diagonal active transition, the upper laser lifetime could be increased, which eventually improved the slope efficiency and decreased the threshold current density. A diagonal transition QCD has generally a smaller overlap of the wave-functions of the active energy levels, where the non-optical scattering rate between the two levels is reduced, which enhances the extraction efficiency and resistance. This leads to an improved overall performance, even though the absorption strength of the active transition is smaller, compared to a vertical transition. Since the extraction of the diagonal transition QCD is not based on resonant tunneling, it does not require such careful alignment and is fundamentally more robust.

A standard QCD consists of one active well with two energy levels for the optical transition and an extractor that is strongly coupled to the upper energy level of the active well. Figure 1(a) shows the band-diagram for the standard QCD with the highest demonstrated responsivity in the wavelength range around 8 μm, which is used as the reference design (N1021).[8] The optical transition happens between the energy levels indicated by the black arrows. Since the extraction is based on resonant tunneling, such a scheme is very sensitive to the alignment between the first extractor level and the upper level of the active transition. Small variations can be compensated by applying a little bias voltage, however, always at the cost of an increased noise. In order for an excited electron to contribute to the photocurrent, it needs to reach the ground level of the next cascade. The extractor must be designed such that the preferential transport direction of electrons is towards this lower active level of the next cascade. Usually, aiming for the highest possible extraction leads to a low resistance and thus high noise. For QCDs, operating at zero bias, the dominant noise mechanism is Johnson noise, which is, for a current source, indirect proportional to the device resistance. Thus, there is a tradeoff between extraction efficiency and resistance. The scattering rate of LO-phonons is in good approximation proportional to the overlap integral (OI) of the participating energy levels. For a vertical transition, as in the reference design, the overlap is high and thus LO-phonon scattering from the upper state back into the lower

a)Electronic mail: peter.reininger@tuwien.ac.at

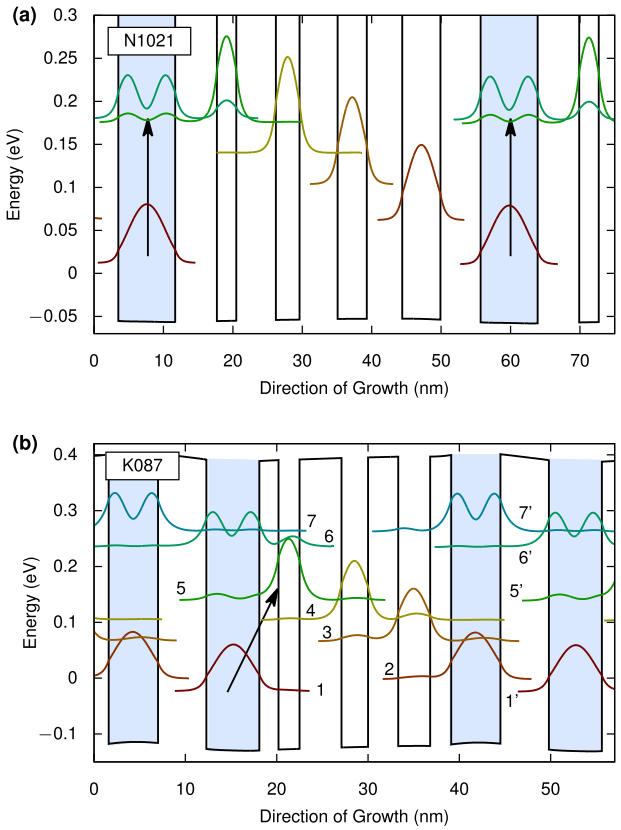

FIG. 1. The bandstructure of the N1021 and K087 samples. The optical transitions are indicated by the black arrows. An electron is excited from the lower to the upper state. From there, it can escape into the extractor, eventually reaching the ground level of the next cascade and contributing to the photocurrent. The optical transition of the standard QCD happens between two energy levels in one well, while the optical transition of the diagonal QCD occurs between two energy levels in different wells. (a) The N1021 sample from Ref. 8. The layer thicknesses of (b) in nm are **2.3**/5.4/**5.3**/5.8/**2.1**/2.3/**4.6**/2.9/**3.3**/3.5 with the first underlined layer doped at $n = 8 \times 10^{17}\,\mathrm{cm}^{-3}$ and the second at $n = 12 \times 10^{17}\,\mathrm{cm}^{-3}$. The Barriers are indicated in bold.

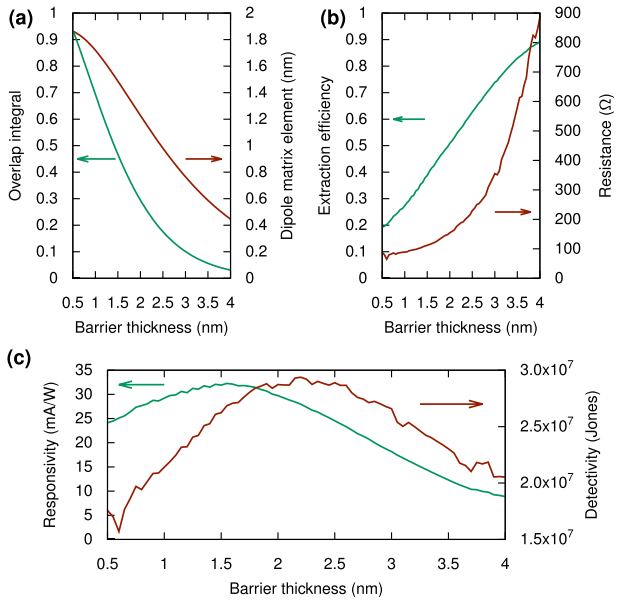

FIG. 2. (a) OI and DME over the barrier thickness between the two active wells. At 0.5 nm, an initial increase of the barrier thickness results in a much steeper drop of the OI than the DME, yielding a overall performance increase. At approximately 2.5 nm, the case begins to reverse and the overall performance drops. (b) Extraction efficiency p_e and resistance of a $100 \times 100\,\mu$m mesa. (c) Responsivity and detectivity.

active level limits the extraction efficiency and reduces the resistance.

The diagonal transition QCD is based on a transition from an energy level localized in one well to an energy level that is localized in the neighboring well. Figure 1(b) shows the band-diagram of the diagonal transition design. The black arrow indicates the optical transition between energy levels 1 and 5. According to our simulations, 35% of the carriers are located in the final well of the extractor (5.4 nm well) and 60% in the broad active well. In order to counteract band-bending, the doping has been distributed in those two wells, as indicated by the shaded blue areas. The second energy level in the broad active well (indicated as 6), has an absorption strength of the same magnitude as the designed transition, but a lower extraction efficiency. Since the transition energy between level 1 and 5 can be designed, to a certain point, separately from 1 to 6, two absorption frequencies can be specifically tuned for dual-color applications. The most important design parameter is the barrier between the two active wells. Figure 2(a) shows the DME and the OI of the optical transition over the thickness of the barrier between the two active wells. Starting at 0.5 nm, an initial increase of the barrier thickness results in a much steeper drop of the OI than the DME, yielding a total performance increase. At approximately 2.5 nm, it reaches its optimal value. Considering only the DME, the highest absorption can be expected for a small barrier thickness. However, Figure 2(b) shows that at such thicknesses both the extraction efficiency and the resistance are low. Because of this trade off, optimization is accomplished by maximizing the output current per unit of input signal power, i.e., the responsivity R_p. For QCDs the responsivity can be written as

$$R_p = \frac{\lambda q}{hc}\frac{\eta\, p_e}{N}, \tag{1}$$

where λ is the wavelength, q the elementary charge, h is the Planck constant, c is the vacuum speed of light, η is the absorption efficiency, which is in good approximation proportional to the squared DME, p_e the extraction efficiency, and N the number of QCD cascades. Another common figure of merit for photodetectors is the specific detectivity D_j^*, which contains terms for both, the signal strength and the noise. The detectivity is defined as

$$D_j^* = R_p \sqrt{\frac{R_0 A}{4 k_B T}}, \tag{2}$$

where R_0 is the resistance, A the optical area, k_B is the Boltzmann constant, and T the temperature. Figure 2(c) shows the responsivity and the detectivity of the device over the barrier thickness. At around 1.5 nm, the responsivity reaches its peak value. The maximum detectivity is at a larger barrier thickness of around 2.1 nm.

A standard QCD is heavily reliant on the alignment of the upper active state and the extractor. To produce a good device, the material parameters must be well known and the growth well controlled. Although that is not an issue for well

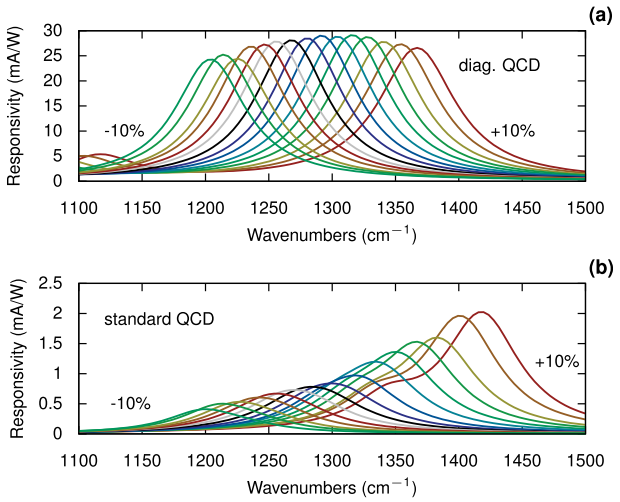

FIG. 3. Responsivity spectrum of (a) the diagonal QCD and (b) the standard QCD for different scaled active region thicknesses. The total active region thicknesses were scaled from −10% to +10%. The diagonal transition QCDs performance is robust against thickness variations. The standard QCD performance drops significantly. The absorption frequency shifts for both devices. The total shift in energy is approximately 170 cm^{-1} for the diagonal transition and 240 cm^{-1} for the standard QCD.

established material systems such as InGaAs/InAlAs or GaAs/AlGaAs, studying new material systems often results in a wide variance of grown structures. The diagonal transition QCD is a more robust design. Figure 3 shows the calculated responsivity spectrum for a distribution of devices with different scaled total active region thicknesses, going from −10% to +10%. Since all wells and barriers, including the active wells, are scaled, the transition energy will scale accordingly. The total shift in energy is approximately 170 cm^{-1} for the diagonal transition and 240 cm^{-1} for the standard QCD. Even at ±10% the performance of the diagonal QCD (a) is hardly influenced, while the responsivity of the reference design (b) clearly shows a strong dependence on the scaling factor.

The simulations were performed with a semi-classical Monte-Carlo transport simulator, which is part of the Vienna Schrödinger Poisson (VSP) framework.[16] The material system of the designed structure is lattice matched InGaAs/InAlAs on InP. All samples were grown by molecular beam epitaxy on semi-insulating InP substrates. The 30 cascades of the QCD are sandwiched between a 600 nm Si-doped InGaAs bottom contact layer and a 200 nm Si-doped InGaAs top contact layer. The processing of the devices starts with the definition of the mesa by lithography and wet-chemical etching with H_3PO_4:H_2O_2:H_2O (1:4:1). Then, bottom and top contacts are defined by lithography, Ge/Au/Ni/Au evaporation, and lift-off. To measure the spectral response, a Fourier-transform infrared spectrometer was used with a Globar broadband light source. The mesa devices were illuminated through a 45° polished facet.

Figure 4 shows the measured photocurrent spectra for different temperatures. Two strong peaks are visible. The first peak at 1250 cm^{-1} comes from the optical transition between energy levels 1 and 5. The second peak at 2150 cm^{-1} can be attributed to the transition between energy levels 1 and 6. It must be pointed out that for the spectral

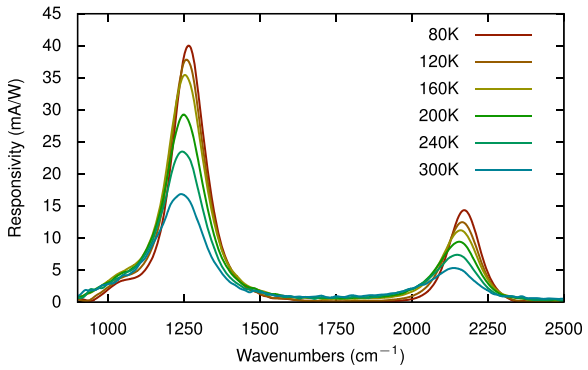

FIG. 4. Measured photocurrent spectrum of the diagonal transition QCD sample K152. The peak at 1250 cm^{-1} comes from the optical transition between energy level 1 and 5, the bump at 1050 cm^{-1} from a small overlap between levels 1 and 4. The second peak at 2150 cm^{-1} can be accounted to the transition between energy levels 1 and 6.

measurements, in this setup, we aligned for the maximum photocurrent. We have observed that by altering the optical alignment, the relative heights of the peaks to each other can be changed. A peak responsivity of 16.9 mA/W for 8 μm was measured at room-temperature.

In conclusion, this work reports the diagonal transition QCD. A design concept where the active transition of the detectors takes place between two energy levels, each localized in different, but adjacent wells. By tuning the barrier between the two wells, the responsivity or the resistance can be optimized to fit specific applications. Since the diagonal transition design does not rely on resonant tunneling, it is more robust compared to a standard QCD. The presented simulations showed that even for a 10% thicker or thinner structure, the responsivity only drops roughly 12%. A responsivity improvement of almost one order of magnitude was demonstrated with a measured peak responsivity of 16.9 mA/W.

The authors acknowledge the support by the Austrian Science Funds (FWF) in the framework of the Doctoral School "Building Solids for Function" (Project W1243), the Project NextLite (SFB F49-09), and the FP7 EU-Project ICARUS.

[1]H. Schneider, C. Schönbein, G. Bihlmann, P. Van Son, and H. Sigg, Appl. Phys. Lett. **70**, 1602 (1997).
[2]H. Schneider and H. C. Liu, *Quantum Well Infrared Photodetectors* (Springer, Berlin, 2006).
[3]D. Hofstetter, M. Beck, and J. Faist, Appl. Phys. Lett. **81**, 2683 (2002).
[4]M. Graf, G. Scalari, D. Hofstetter, J. Faist, H. Beere, E. Linfield, D. Ritchie, and G. Davies, Appl. Phys. Lett. **84**, 475 (2004).
[5]M. Graf, N. Hoyler, M. Giovannini, J. Faist, and D. Hofstetter, Appl. Phys. Lett. **88**, 241118 (2006).
[6]L. Gendron, M. Carras, A. Huynh, V. Ortiz, C. Koeniguer, and V. Berger, Appl. Phys. Lett. **85**, 2824 (2004).
[7]L. Gendron, C. Koeniguer, V. Berger, and X. Marcadet, Appl. Phys. Lett. **86**, 121116 (2005).
[8]F. R. Giorgetta, E. Baumann, M. Graf, Q. Yangi, C. Manz, K. Köhler, H. E. Beere, D. Ritchie, E. Linfield, A. G. Davies, Y. Fedoryshyn, H. Jäckel, M. Fischer, J. Faist, and D. Hofstetter, IEEE J. Quantum Electron. **45**, 1039 (2009).
[9]H. Liu, C. Song, A. J. S. Thorpe, and J. Cao, Appl. Phys. Lett. **84**, 4068 (2004).
[10]S. Sakr, E. Giraud, A. Dussaigne, M. Tchernycheva, N. Grandjean, and F. H. Julien, Appl. Phys. Lett. **100**, 181103 (2012).

[11]D. Hofstetter, F. R. Giorgetta, E. Baumann, Q. Yang, C. Manz, and K. Köhler, Appl. Phys. Lett. **93**, 221106 (2008).
[12]P. Reininger, B. Schwarz, A. Harrer, T. Zederbauer, H. Detz, A. M. Andrews, R. Gansch, W. Schrenk, and G. Strasser, Appl. Phys. Lett. **103**, 241103 (2013).
[13]B. Schwarz, P. Reininger, H. Detz, T. Zederbauer, A. M. Andrews, S. Kalchmair, W. Schrenk, O. Baumgartner, H. Kosina, and G. Strasser, Appl. Phys. Lett. **101**, 191109 (2012).
[14]B. Schwarz, P. Reininger, D. Ristanić, H. Detz, A. M. Andrews, W. Schrenk, and G. Strasser, Nat. Commun. **5**, 4085 (2014).
[15]P. Q. Liu, A. J. Hoffman, M. D. Escarra, K. J. Franz, J. B. Khurgin, Y. Dikmelik, X. Wang, J.-Y. Fan, and C. F. Gmachl, Nat. Photonics **4**, 95 (2010).
[16]O. Baumgartner, Z. Stanojevic, and H. Kosina, in *Proceedings of the International Conference on Simulation of Semiconductor Processes and Devices (SISPAD)* (Osaka, 2011), p. 91.